[10]Tumin, A., "A Model of Spatial Algebraic Growth in a Boundary Layer Subjected to a Streamwise Pressure Gradient," *Physics of Fluids*, Vol. 13, 2001, pp. 1521–1523.

[11]Reshotko, E., and Tumin, A., "Investigation of the Role of Transient Growth in Roughness-Induced Transition," AIAA Paper 2002-2850, June 2002.

[12]Volino, R. J., "Separated Flow Transition Under Simulated Low-Pressure Turbine Airfoil Conditions: Part 1—Mean Flow and Turbulence Statistics," *Proceedings of the ASME TURBO EXPO 2002* [CD-ROM], American Society of Mechanical Engineers, Paper GT-2002-30236, 2002.

A. Plotkin
Associate Editor

In Situ Calibration Uncertainty of Pressure-Sensitive Paint

Tianshu Liu*
NASA Langley Research Center, Hampton, Virginia 23681-2199
and
John P. Sullivan†
Purdue University, West Lafayette, Indiana 47906

Introduction

PRESSURE-SENSITIVE paint (PSP) is an optical sensor for measuring surface pressure distributions on wind-tunnel models.[1,2] Because of oxygen quenching of luminescence, the luminescent intensity I emitted from PSP is related to air pressure p by the linear Stern–Volmer relation over a certain range:

$$I_{\text{ref}}/I = A(T) + B(T)(p/p_{\text{ref}}) \tag{1}$$

where I_{ref} and p_{ref} are the reference luminescent intensity and pressure at a known temperature, respectively. The Stern–Volmer coefficients $A(T)$ and $B(T)$ are temperature dependent because temperature affects both nonradiative deactivation and oxygen diffusion in a polymer. In principle, a priori calibration of PSP in a pressure cell can be used for conversion from the luminescent intensity to pressure using Eq. (1). However, this approach often leads to a considerable systematic error because the surface temperature distribution is not known and the illumination change on surface due to model deformation cannot be corrected by image registration. The systematic error is also related to uncontrollable environmental testing factors. Therefore, in actual PSP measurements, experimental aerodynamicists calibrate PSP in situ by fitting (or correlating) the normalized luminescent intensity to pressure tap data at a number of distributed locations. In a sense, in situ PSP calibration eliminates the systematic error associated with the temperature effect and the illumination change by absorbing it into the overall fitting error. In situ PSP calibration uncertainty is not sufficiently discussed, although Sajben[3] and Liu et al.[4] have given a general uncertainty analysis of PSP. Recently, Kammeyer et al.[5,6] assessed the accuracy of The Boeing Company production PSP system by statistical analysis of comparison between PSP and pressure transducers over a large numbers of data points on a 1/12th-scale model of a Cessna Citation. Tests were run at several Mach numbers from 0.22 to 0.82, two Reynolds numbers of 4.5 and 8.3×10^6, and 14 angles of attack ranging from −4 to 10 deg. Kammeyer et al. found that in situ calibration error was a function of the angle of attack (AOA) and Mach number. It was also found that the histogram of the overall set of in situ PSP errors obtained at all of the Mach numbers and AOA exhibited a distinct non-Gaussian distribution. In this Note, we study in situ calibration uncertainty of PSP through a simulation of PSP measurements in subsonic Joukowsky airfoil flows where in situ calibration uncertainty is mainly attributed to the temperature effect of PSP and illumination change on surface due to model deformation. The simulation complements the experimental results obtained by Kammeyer et al.[5,6] providing useful insights to in situ calibration uncertainty of PSP.

Simulated In Situ PSP Calibration in Subsonic Joukowsky Airfoil Flows

Hypothetical PSP measurements on a Joukowsky airfoil in subsonic flows are considered to estimate in situ PSP calibration uncertainty. The airfoil and incompressible potential flows around it are generated using the Joukowsky transform. The pressure coefficients on the airfoil in the corresponding subsonic compressible flows are obtained using the Kármán–Tsien rule. We consider an adiabatic model at which the adiabatic wall temperature T_{aw} is given by $T_{\text{aw}}/T_0 = [1 + r(\gamma - 1)M^2/2][1 + (\gamma - 1)M^2/2]^{-1}$. The recovery factor is $r = 0.843$ for a laminar boundary layer on the airfoil. Assuming that the reference temperature T_{ref} in the wind-off case equals to the total temperature of the flow $T_0 = 293$ K, we can calculate the temperature difference $\Delta T = T_{\text{aw}} - T_{\text{ref}}$ between the wind-on and wind-off cases. Figure 1 shows typical distributions of the pressure coefficient C_p and adiabatic wall temperature T_{aw} on a Joukowsky airfoil at AOA = 5 deg and Mach 0.4. The airfoil has a 25% thickness and 2% camber relative to the chord.

In an object–space coordinate system whose origin is located at the leading edge of the airfoil, four light sources for illuminating PSP are placed at the locations $\boldsymbol{X}_{s1} = (-\bar{c}, 3\bar{c})$, $\boldsymbol{X}_{s2} = (2\bar{c}, 3\bar{c})$, $\boldsymbol{X}_{s3} = (-\bar{c}, -3\bar{c})$, and $\boldsymbol{X}_{s4} = (2\bar{c}, -3\bar{c})$, where $\bar{c}$ is the chord of the airfoil. When a light is modeled as a point light source with unit strength, distributions of the illumination radiance on the upper and lower surfaces of the airfoil are

$$L_{\text{up}} = |\boldsymbol{X}_{\text{up}} - \boldsymbol{X}_{s1}|^{-2} + |\boldsymbol{X}_{\text{up}} - \boldsymbol{X}_{s2}|^{-2}$$
$$L_{\text{low}} = |\boldsymbol{X}_{\text{low}} - \boldsymbol{X}_{s3}|^{-2} + |\boldsymbol{X}_{\text{low}} - \boldsymbol{X}_{s4}|^{-2} \tag{2}$$

where $\boldsymbol{X}_{\text{up}}$ and $\boldsymbol{X}_{\text{low}}$ are the coordinates of the upper and lower surfaces of the airfoil, respectively. Two cameras, viewing the upper

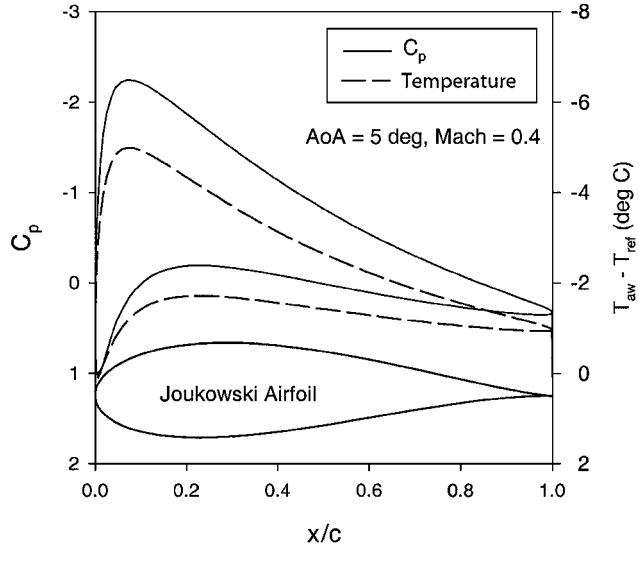

Fig. 1 Typical distributions of the pressure coefficient C_p and the adiabatic wall temperature T_{aw} on a Joukowski airfoil.

Received 5 December 2002; revision received 5 June 2003; accepted for publication 9 June 2003.

*Research Scientist, Aerodynamics, Aerothermodynamics and Acoustics Competency, Mail Stop 238; t.liu@larc.nasa.gov. Member AIAA.

†Professor, School of Aeronautics and Astronautics. Member AIAA.

surface and lower surface from the normal direction to the airfoil, are located at $(\bar{c}/2, 4\bar{c})$ and $(\bar{c}/2, -4\bar{c})$, respectively.

Aerodynamic load produces elastic wing deformation composed of twist and bending, while the local wing airfoil section remains unchanged.[7] Therefore, the local movement of the airfoil at a spanwise location can be described by a superposition of a rotation (twist) and a translation. At a spanwise location, the local transformation from the nondeformed surface coordinates $\boldsymbol{X} = (X, Y)^T$ to the deformed coordinates $\boldsymbol{X}' = (X', Y')^T$ is

$$\boldsymbol{X}' = \begin{pmatrix} \cos\theta_{\text{twist}} & \sin\theta_{\text{twist}} \\ -\sin\theta_{\text{twist}} & \cos\theta_{\text{twist}} \end{pmatrix} \boldsymbol{X} + \boldsymbol{T} \tag{3}$$

where θ_{twist} is the local wing twist and $\boldsymbol{T} = (0, T_y)^T$ is the translation vector assuming the translation in the x direction is zero. The wing bending is usually given by T_y as a function of the spanwise coordinate. Both the twist θ_{twist} and bending T_y are a function of AOA α for a given Mach number and Reynolds number. Based on previous wing deformation measurements,[7] we use the typical linear relations $\theta_{\text{twist}} = -0.113\alpha$ (deg) and $T_y = 0.022\alpha$ (in.) [0.559α (mm)] over a certain range of AOA. Thus, using Eqs. (2) and (3), we can estimate a change of the illumination radiance on the airfoil surface due to deformation.

Presumably, a typical PSP, bathophen ruthenium chloride plus silica gel in GE RTV 118, is used,[4] which has the temperature-dependent Stern–Volmer coefficients $A(T) \approx 0.13[1 + 2.82(T - T_{\text{ref}})/T_{\text{ref}}]$ and $B(T) \approx 0.87[1 + 4.32(T - T_{\text{ref}})/T_{\text{ref}}]$ over a temperature range of 293–333 K. In simulations, the measured luminescent intensity I distribution of PSP in the wind-on case (deformation case) is generated by

$$\begin{aligned} I/I_{\text{ref0}} &= (I_{\text{ref}}/I_{\text{ref0}})[A(T) + B(T)(p/p_{\text{ref}})]^{-1} \\ &= (L/L_0)[A(T) + B(T)(p/p_{\text{ref}})]^{-1} \end{aligned} \tag{4}$$

where I_{ref0} and I_{ref} are the reference luminescent intensities (without wind) on the nondeformed airfoil and deformed airfoil, respectively. Equation (4) assumes that I_{ref0} and I_{ref} are proportional to the corresponding illumination radiance levels L_0 and L on the nondeformed airfoil and deformed airfoil, respectively. The illumination radiance levels L_0 and L in Eq. (4) can be calculated using Eq. (2) coupled with Eq. (3). In Eq. (4), the surface temperature T is substituted by the adiabatic wall temperature distribution T_{aw}, and the pressure distribution is given by the Joukowsky transform plus the Kármán–Tsien rule for subsonic flows. Therefore, the resulting luminescent intensity distribution given by Eq. (4) contains effects of both the illumination change and temperature variation on the surface.

When it is assumed that the wind-on image I is already aligned with the wind-off image I_{ref0} on the nondeformed airfoil by image registration, in situ PSP calibration is made to correlate I_{ref0}/I to p/p_{ref} using the Stern–Volmer relation. Figure 2 shows typical in situ PSP calibrations on the upper and lower surfaces of the airfoil for AOA = 5 deg and Mach 0.4, where 104 virtual pressure taps are used for each of the upper and lower surfaces. The in situ calibration curves on the upper and lower surfaces are different due to the significant temperature difference and change of the illumination level on the surfaces. Figure 3 shows a histogram of the normalized in situ calibration error $\Delta p/p_{\text{ref}} = (p - p_{\text{in situ}})/p_{\text{ref}}$ in this case, where Δp is a difference between the true pressure from the theoretical distribution and the pressure converted from the luminescent intensity using in situ calibration. For a given AOA and Mach number, the histogram of in situ calibration error exhibits a near-Gaussian distribution. The standard deviation of the probability density function is dependent on AOA and Mach number. Figures 4 and 5 show the standard deviation of in situ calibration error as a function of AOA for Mach 0.4 and as a function of Mach number for AOA = 5 deg, respectively. The isolated effect of the temperature and illumination change on the standard deviation is also shown in Figs. 4 and 5. The behavior of the calculated standard deviation as a function of AOA and Mach number is very similar to the experimental results obtained by Kammeyer et al.[5,6] The concavity of the standard deviation as a function of AOA in Fig. 4 is mainly attributed to the movement of the airfoil.

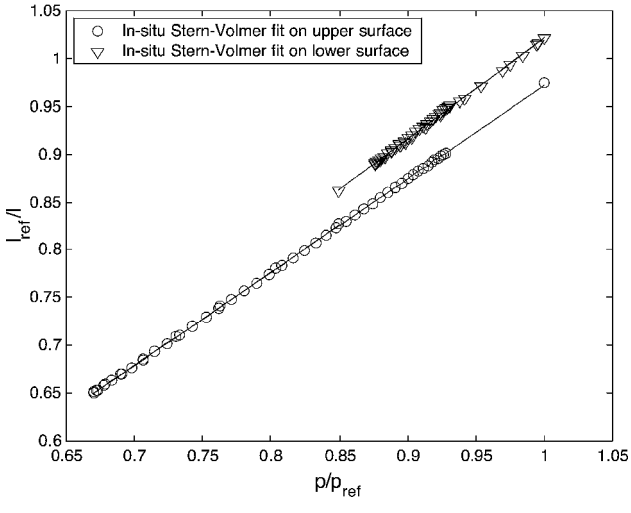

Fig. 2 In situ PSP calibration on a Joukowski airfoil at AOA = 5 deg and Mach 0.4.

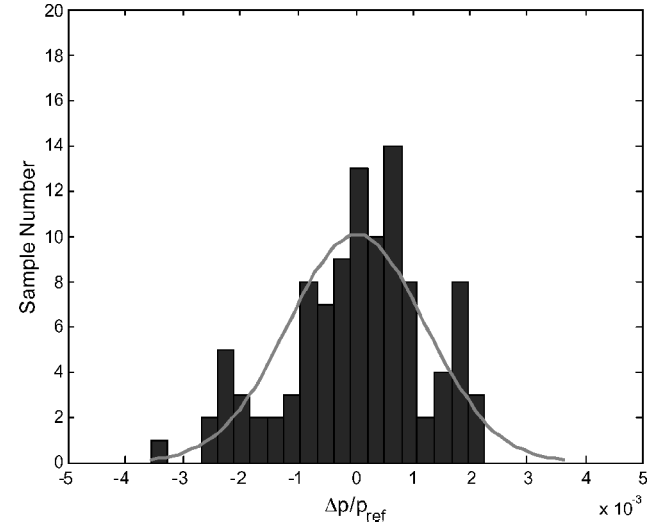

Fig. 3 Histogram of in situ PSP calibration error on a Joukowski airfoil at AOA = 5 deg and Mach 0.4.

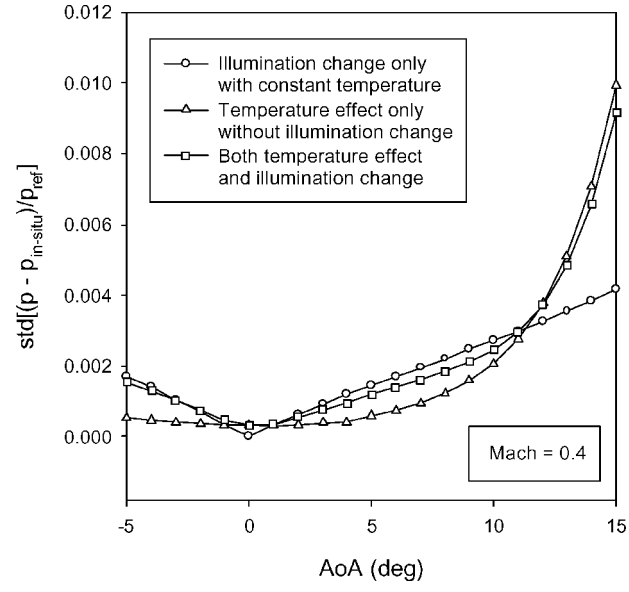

Fig. 4 Standard deviation of in situ PSP calibration error as a function of AOA at Mach 0.4.

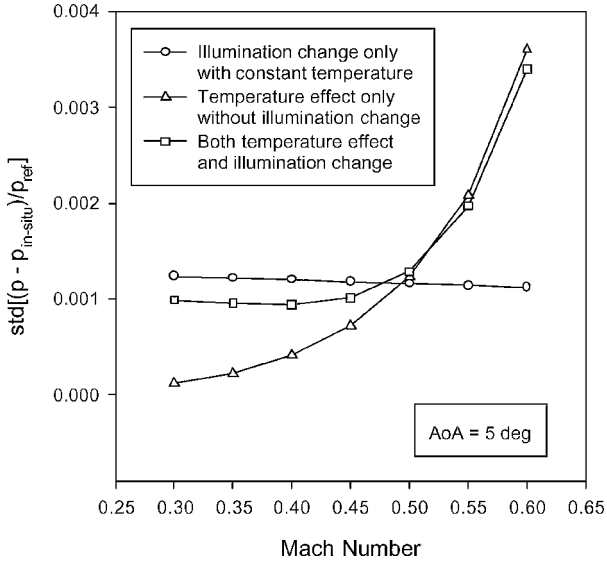

Fig. 5 Standard deviation of in situ PSP calibration error as a function of Mach number at AOA = 5 deg.

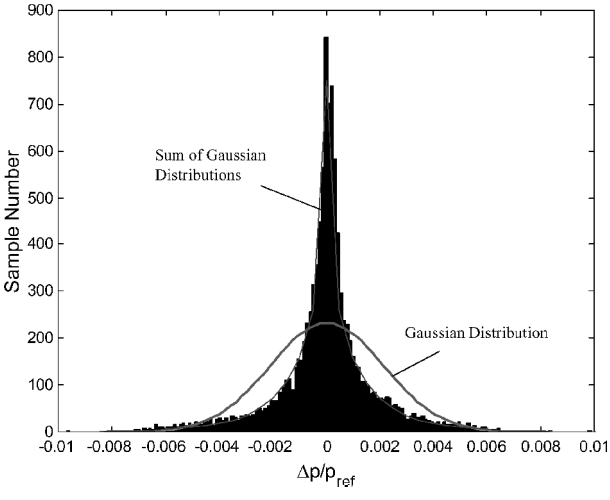

Fig. 6 Histogram of a union of all sample sets of in situ PSP calibration error over the whole range of AOA and Mach numbers.

Kammeyer et al.[5,6] found that the histogram of in situ calibration error was non-Gaussian for the overall set of samples over the whole range of AOA and Mach numbers. Figure 6 shows the simulated distribution for an overall set of samples of $\Delta p/p_{\text{ref}}$ (a total of 10,920 samples) over the whole range of AOA and Mach numbers, which duplicates the experimental non-Gaussian distribution given by Kammeyer et al. The Gaussian distribution with the same standard deviation is also plotted in Fig. 6 for comparison. In fact, for a union of sample sets having near-Gaussian distributions with different the standard deviation values at different AOA and Mach numbers, the distribution becomes non-Gaussian because more and more samples accumulate near zero when forming the union of the sample sets. The probability density function of a union of N sample sets is given by a sum of the Gaussian distributions rather than the Gaussian distribution, that is,

$$N^{-1}\sum_{i=1}^{N}\exp\left(\frac{-x^2}{2\sigma_i^2}\right)\Big/\sqrt{2\pi}\sigma_i \qquad (5)$$

As shown in Fig. 6, the distribution Eq. (5) correctly describes the simulated distribution. Note that we should not confuse this case with the central limit theorem that deals with a sum of independent random variables. Although the simulation is made for an airfoil section of a wing, the error for the wing can be estimated by averaging the local results over the full span of the wing. The behavior of the error for the wing should be similar to that for the airfoil.

Conclusions

In situ calibration uncertainty of PSP on the Joukowsky airfoil in subsonic flows is dominated by the temperature effect of PSP and the illumination change on surface due to model deformation, and therefore, it depends on AOA and Mach number. For a given AOA and Mach number, the probability density distribution of errors of in situ calibration conducted on the airfoil is near-Gaussian. However, the distribution becomes highly non-Gaussian for a union of all of the sample sets over the whole range of AOA and Mach numbers, which can be described as a sum of the Gaussian distributions. The simulation is consistent with the experimental results obtained by Kammeyer et al.[5,6]

References

[1]Liu, T., Campbell, B. T., Burns, S. P., and Sullivan, J. P., "Temperature- and Pressure-Sensitive Luminescent Paints in Aerodynamics," *Applied Mechanics Reviews*, Vol. 50, No. 4, 1997, pp. 227–246.

[2]Bell, J. H., Shairer, E. T., Hand, L. A., and Mehta, R. D., "Surface Pressure Measurements Using Luminescent Coatings," *Annual Review of Fluid Mechanics*, Vol. 33, March 2001, pp. 155–206.

[3]Sajben, M., "Uncertainty Estimates for Pressure Sensitive Paint Measurements," *AIAA Journal*, Vol. 31, No. 11, 1993, pp. 2105–2110.

[4]Liu, T., Guille, M., and Sullivan, J., "Accuracy of Pressure-Sensitive Paint," *AIAA Journal*, Vol. 39, No. 1, 2001, pp. 103–112.

[5]Kammeyer, M., Donovan, J., Kelble, C., Benne, M., Kihlken, T., and Felter, J. A., "Accuracy Assessment of a Pressure-Sensitive Paint Measurement System," AIAA Paper 2002-0530, Jan. 2002.

[6]Kammeyer, M., Kelble, C., Donovan, J., Benne, M., and Kihlken, T., "Recent Improvements in Pressure-Sensitive Paint Measurement Accuracy at Boeing," AIAA Paper 2002-2907, June 2002.

[7]Burner, A. W., and Liu, T., "Videogrammetric Model Deformation Measurement Technique," *Journal of Aircraft*, Vol. 38, No. 4, 2001, pp. 745–754.

R. P. Lucht
Associate Editor

Region of Flutter and Buckling Instability for a Cracked Beam

Q. Wang*
University of Central Florida, Orlando, Florida 32816-2450
and
C. G. Koh†
National University of Singapore, Singapore 119260, Republic of Singapore

I. Introduction

ANALYSIS of flutter and buckling of beams has long attracted attention in the applied mechanics community. The mathematical solutions for the critical force of a beam with different boundary conditions subjected to a nonfollower compression were given in the monograph by Timoshenko and Gere.[1] In addition, flutter analysis of a cantilever beam was also briefly conducted in the monograph. Beam buckling is an instability phenomenon referring to change of equilibrium state from one configuration to another one at a critical compression value. On the other hand, flutter is another type of beam instability when the vibration amplitude

Received 3 April 2003; revision received 7 July 2003; accepted for publication 15 July 2003.

*Associate Professor, Mechanical, Materials and Aerospace Engineering Department, 4000 Central Florida Boulevard; qzwang@mail.ucf.edu.

†Associate Professor, Department of Civil Engineering.